Electronic Supplementary Material (ESI) for Journal of Materials Chemistry C.
This journal is © The Royal Society of Chemistry 2024

Electronic Supplementary Information

Heterometallic $\{Re_4Mo_2Q^i_8\}$ Cluster-Based Building Blocks: Towards the Rational Nanoarchitectonics of Optimized Photoelectrodes for Solar Cells and Water Splitting.

Tatiana I. Lappi,[a,b] Stéphane Cordier,[a] Yakov M. Gayfulin,[b] Soraya Ababou-Girard,[c] Ngan T. K. Nguyen,[d,e] Fabien Grasset,[a,d] Tetsuo Uchikoshi,[d,f] Nikolay G. Naumov,[b] and Adèle Renaud[a]**

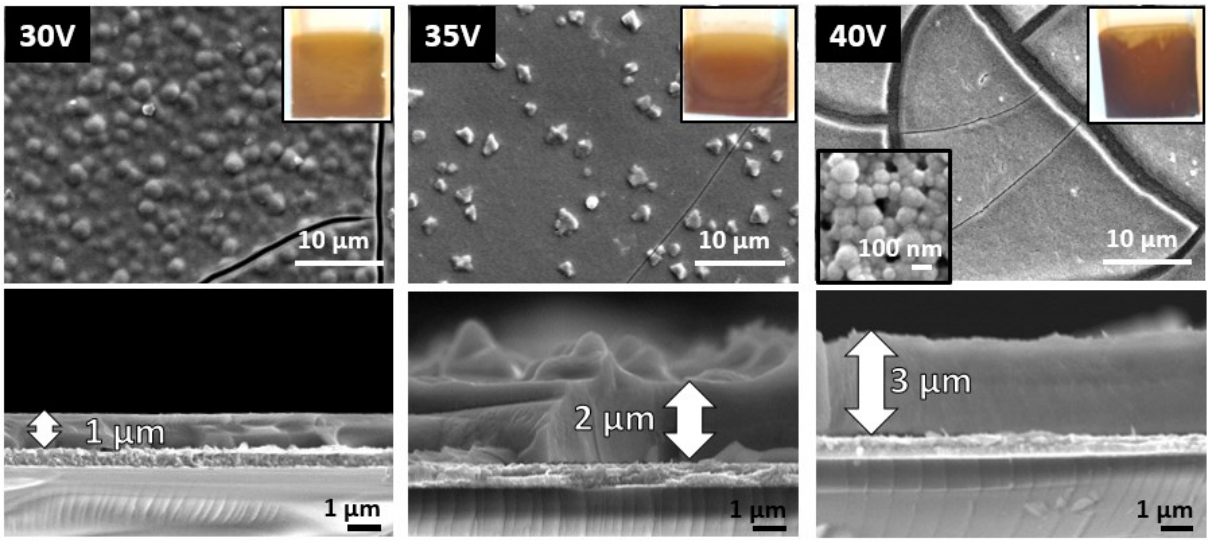

Figure S1. Photographs and SEM images of the top view and the cross sections of the $\{Re_4Mo_2Se_8\}$ cluster-based films deposited at various voltage (from 30 to 40 V) for 30 s.

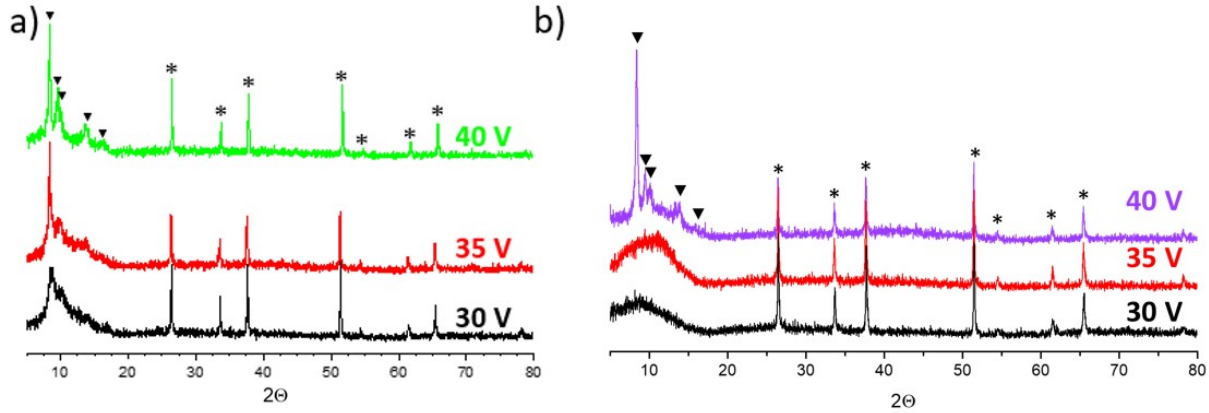

Figure S2. XRD diagrams of a) $\{Re_4Mo_2S_8\}$-based films and b) $\{Re_4Mo_2Se_8\}$-based films according to the applied deposition voltage (from 30V to 40 V). The stars and triangles correspond to FTO substrate and cluster-based film peaks, respectively.

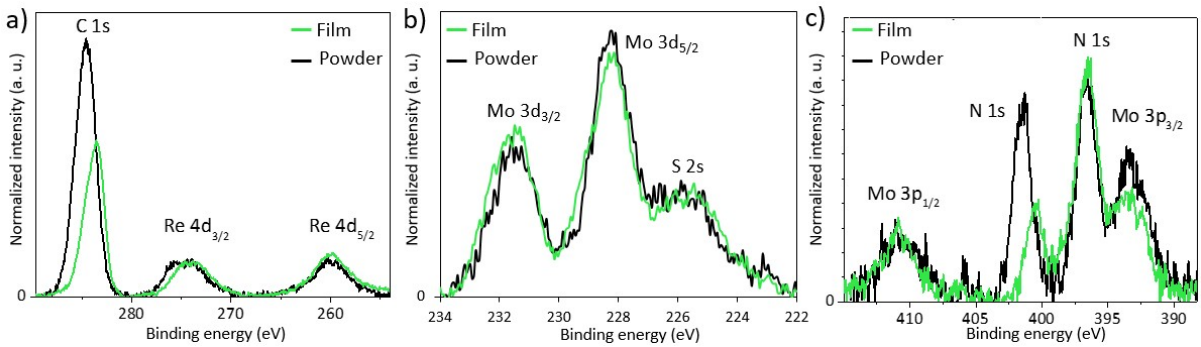

Figure S3. XPS spectra of the $\{Re_4Mo_2S_8\}$-based annealed film and precursor. a) corresponds to Re 4d and C 1s contributions, b) to Mo 3d and S 2s contributions and c) to Mo 3p and N 1s contributions.

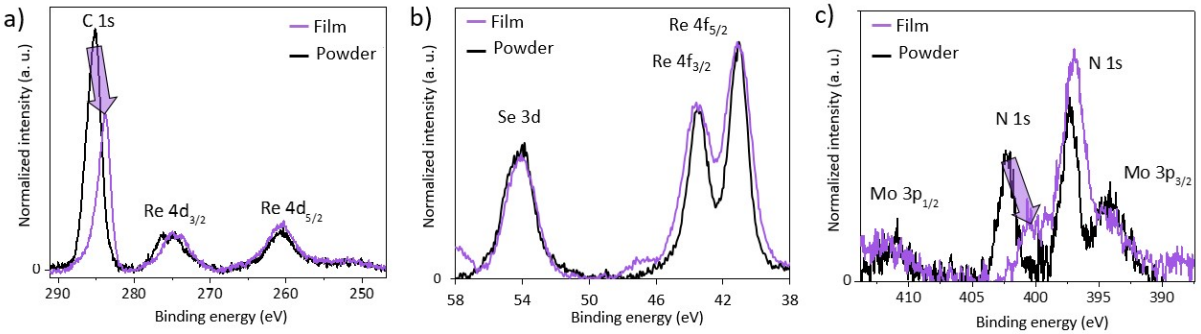

Figure S4. XPS spectra of the $\{Re_4Mo_2Se_8\}$-based annealed film and precursor. a) corresponds to the Re 4d and C 1s contributions, b) to the Re 4f and Se 3d contributions and c) to the Mo 3p and N 1s contributions.

Table S1. Composition of powders **1'** and **2'**, and unheated and heated sulfide and selenide-based films determined by EDS analyses.

Sulfide	S	Mo	Re	Re/Mo	S/(Mo+Re)
Powder (1')	55(3)	17(3)	27(2)	1.5	1.2
Unheated film	61(3)	15(3)	24(2)	1.6	1.5
Annealed film	55(3)	18(3)	27(2)	1.5	1.2
Theoretical composition	**57**	**14**	**29**	**2.0**	**1.3**

Selenide	Se	Mo	Re	Re/Mo	Se/(Mo+Re)
Powder (2')	56(1)	16(1)	28(1)	1.7	1.3
Unheated film	59(1)	18(1)	23(1)	1.3	1.4
Annealed film	58(1)	18(1)	24(1)	1.3	1.4
Theoretical composition	**57**	**14**	**29**	**2.0**	**1.3**

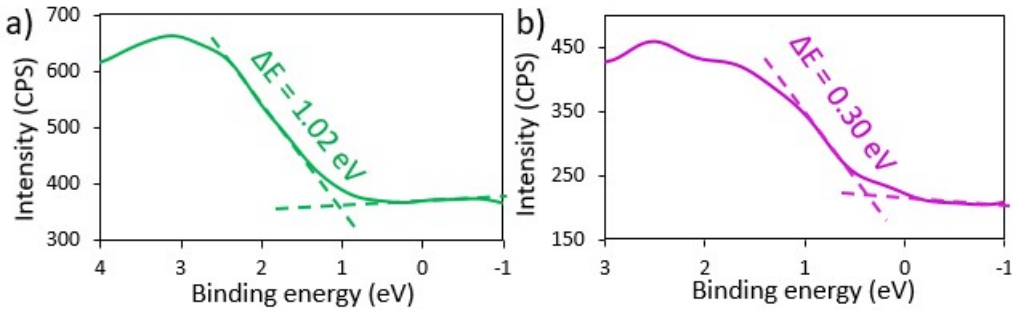

Figure S5. Valence band spectra recorded on annealed a) $\{Re_4Mo_2S_8\}$- and b) $\{Re_4Mo_2Se_8\}$-based annealed films. ΔE corresponds to the energy difference between the valence band maximum (VBM) and the Fermi level (E_F).

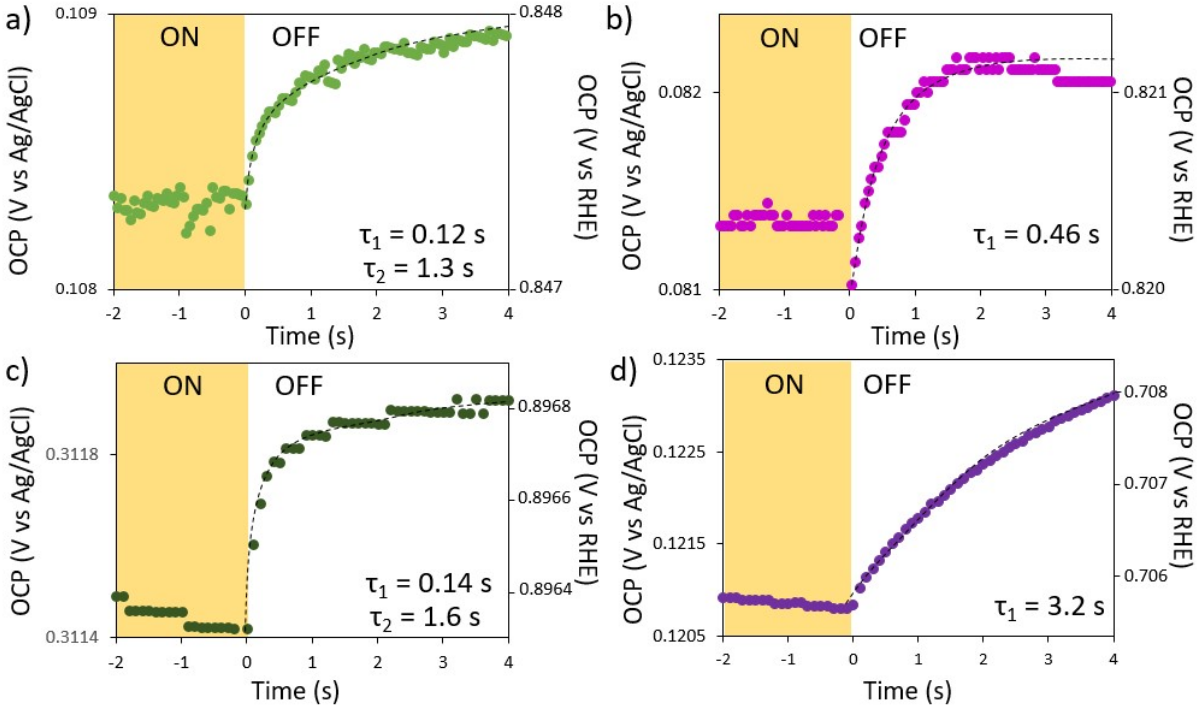

Figure S6. Open circuit potential (OCP) evolution under a chopped illumination of unannealed a) $\{Re_4Mo_2S_8\}$- and b) $\{Re_4Mo_2Se_8\}$- and annealed c) $\{Re_4Mo_2S_8\}$- and d) $\{Re_4Mo_2Se_8\}$-based electrodes.

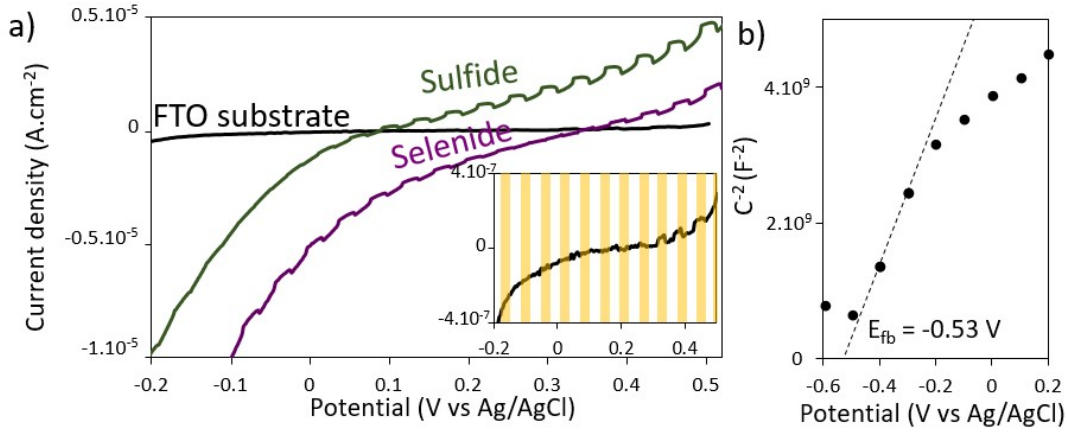

Figure S7. b) Current-potential curves under chopped illumination of the FTO substrate compared to the annealed (T = 200 °C) sulfide (green) and selenide (purple)-based electrodes. The insert correspond to zoom of the FTO signal. b) Mott-Schottky diagram of the FTO substrate and flat band potential determination (electrolyte KCl 0.5 M).

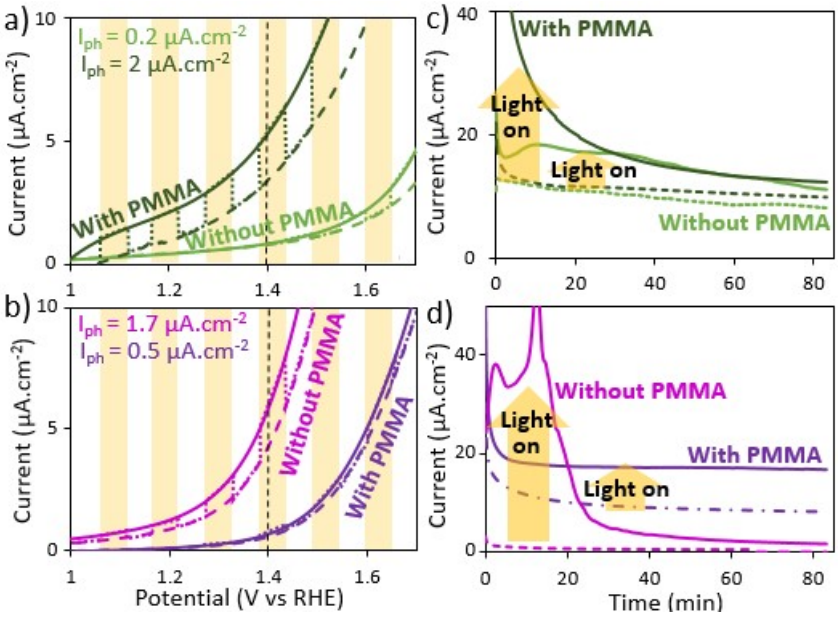

Figure S8. Current-potential curves and chronoamperometry at 1.4 V vs RHE in the dark (dash lines) and under illumination (solid lines) obtained from the annealed (T = 200 °C) a), c) sulfide (green) and b), d) selenide (purple)-based electrodes. a) and b) were obtained under chopped illumination and c) and d) under constant illumination.

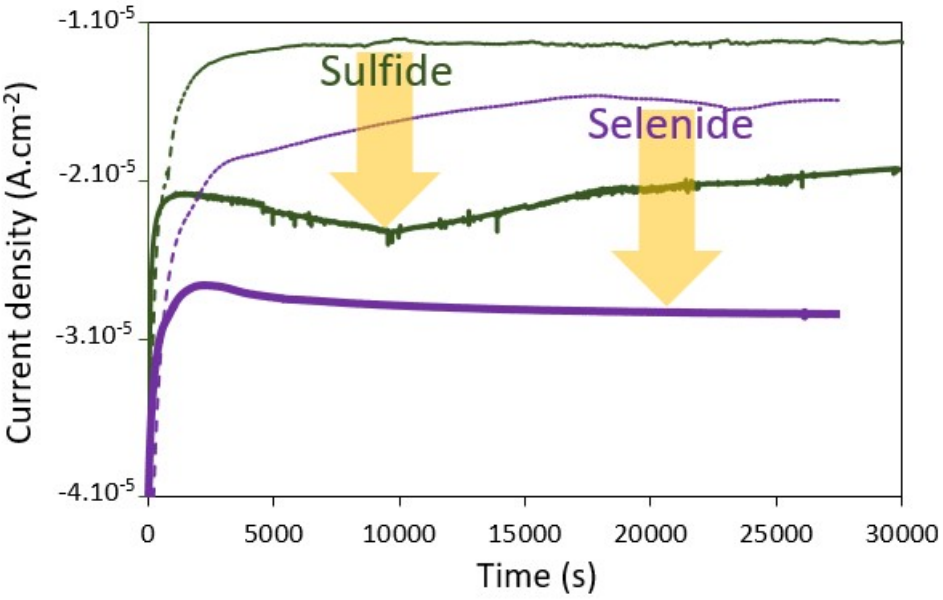

Figure S9. Chronoamperometry at 0.2 V vs RHE in the dark and under illumination obtained from the annealed (T = 200 °C) sulfide (green) selenide (purple)-based electrodes recovered by a PMMA protection.

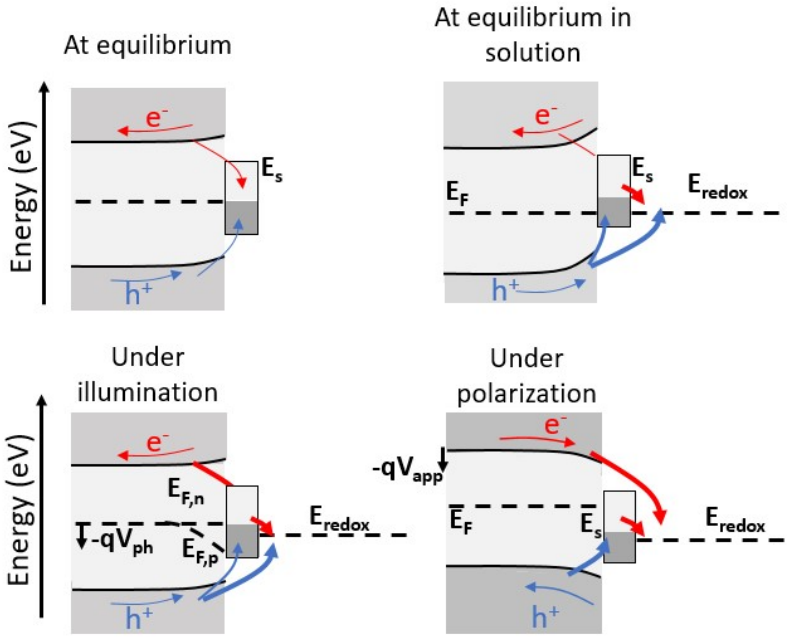

Figure S10. Schematic representation the possible charge pathways at the interface semiconductor/electrolyte influenced by the surface states (Es), and the illumination and polarization conditions. The red and blue arrows correspond to the electrons and holes pathways, respectivement. The size of the arrows is correlated to the flux. Due to the ambipolarity and the proximity between the energy levels in the gap, the illumination and potential applied affect strongly the charge carrier density at the interface.